Stress corrosion cracking of carbon steels on CO_2/H_2O systems

Mariana dos Reis Tagliari [1]*

Pedro Craidy [2]

Derek Fonseca [1]

Marcelo Favaro Borges [1]

Abstract

This review article briefly compiles data available in the literature on cases of stress corrosion cracking on carbon steels in the presence of environments containing CO_2 from a corrosion point of view, seeking to clarify which main factors influence the crack nucleation and propagation. The aspects related to the stress intensity factor and fracture mechanics approach will not be discussed, as well as residual stresses, which are known to be determinant factors in the study of stress corrosion cracking and therefore deserve individual reviews. It will discuss stress corrosion cracking in high strength carbon steels with a brief description of this system´s corrosion mechanisms under study and the main variables involved. Methods for assessing the susceptibility of materials to SCC will also be addressed in the form of results obtained by other authors. Also, it seeks to warn about the care in dealing with the subject, given the variation of parameters in the environment that are influential in the outbreak and spread of the phenomenon. Finally, tests will be commented on to verify the susceptibility to the phenomenon and a brief description of the known cracking mechanisms.

Keywords: Stress corrosion cracking; CO_2/H_2O; High strength carbon steels.

1 Introduction

Stress corrosion cracking of carbon steels in aqueous environments containing CO and CO_2 acquired technological importance since the 60s due to failures in components used to storage and transport pressurized CO_2 [1]. In the CO_2-H_2O system, in the absence of CO, pioneering research such as from Hudgins et al. [2] observed that cracking would be verified only in extreme operational conditions: high-stress levels applied on high strength steels and under high partial pressures of CO_2. Carbon monoxide influences the formation of the passive layer and hydrogen generation, so the CO-CO_2-H_2O system can be considered the most critical.

The corrosion of carbon steels in environments containing CO_2 generates a corrosion product called Siderite ($FeCO_3$) that can be passive or not, depending on the environmental conditions such as pH, brine chemistry such iron and carbonate concentrations, stage of growth, among others [3,4]. This compound can be strongly adherent to the steel substrate and highly compacted. When this layer is disturbed, mechanically, or by chemical dissolution, it can lead to steel substrate exposure and evolve to localized corrosion such as corrosion pit formation [5]. Since corrosion pits are stress raisers, cracks can be nucleated and propagated by different regimes that are dependent on several variables [6-8]. Then extra attention should be given when studying stress-cracking

in CO_2 atmospheres based on the literature available, once in its majority, some variables as dissolved iron and oxygen contents are not even mentioned, and they can substantially affect the intensity of damage [9,10].

This paper reviews the literature regarding stress corrosion cracking on CO_2/H_2O systems. Related failure cases are reported, and relevant test results on CO_2-H_2O systems to assess the susceptibility of this phenomena for carbon and low alloy steels.

2 Definition of stress corrosion cracking

Stress corrosion cracking (SCC) is a degradation process that affects the integrity of metals and alloys. These phenomena occur when three factors are coexisting: a material that contains elements in the alloy making the material susceptible; sufficient tensile stress higher than a threshold value, and finally, an environment. Depending on the resulting combination of variables in the system in question, catastrophic failures can occur. It can be difficult to define one specific mechanism to describe the CO2- assisted SCC phenomenon. The term SCC- CO_2 will be used along with the text, referring to stress corrosion cracking caused by CO_2 [11].

[1]Laboratório de Metalurgia Física – LAMEF, Universidade Federal do Rio Grande do Sul – UFRGS, Porto Alegre, RS, Brasil.

[2]Centro de Pesquisas, Desenvolvimento e Inovação Leopoldo Américo Miguez de Mello – CENPES, Petróleo Brasileiro S.A. – Petrobras, Rio de Janeiro, RJ, Brasil.

*Corresponding author: mreis@ufrgs.br

The term stress corrosion cracking (SCC) is being attributed in this paper to crack propagation due to anodic reactions at the crack tip, considering that the crack propagates due to the material´s consumption by corrosion combined with an elevated K value (stress intensity factor). In many cases, SCC occurs when there is bit visible evidence of general corrosion on the metal surface and is commonly associated with metals that exhibit substantial passivity [11].

3 Failure cases on CO_2/H_2O system

Stress corrosion cracking of carbon steels in aqueous solutions containing CO_2 was studied in the past, and it was verified that the $CO-CO_2-H_2O$ system could promote SCC in low allow carbon steels. Rhodes in the 80s mentioned the occurrence of failures in tubings used for gas injection in wells [12]. Kunze reported failures of 42 cylinders containing CO_2 and H_2O used for storage and transport in the 70s [13], where cracks generally propagated intergranular and were nucleated at corrosion pits and alveolus at the inner surface of the cylinders as showed in Figure 1. The materials with higher mechanical strength show more susceptibility to cracking compared to lower strength materials.

Spahn reported a steel cylinder´s failure in the 70s [14] (UTS 790MPa, YS 685 MPa) operating at 80 to 100 bar of CO_2 after nine years in operation. The water presence (electrolyte) came from an inadequate drying operation after a hydrostatic test before the operation. Recently, in 2012, other authors reported similar failures on cylinders operating at higher pressures, which failed after only three years by intergranular cracking [15].

In 2010 Sadeghi Meresht et al. [16] reported SCC cracks nucleated on active defects at the external surface of an API X60 pipeline operating with high pressures and immersed in CO_3^{2-}/HCO_3^- soil environment with high pH (resulted from the dissociation of CO_2 in water, both present in the soil), that failed the pipe. Colonies of intergranular SCC were observed during failure analysis. Other carbonate-related failures in buried high strength gas transmission pipelines were reported in the literature [17-20].

4 Parameters that affect CO_2 - stress corrosion cracking

Several environmental aspects influence the occurrence of SCC-CO_2. According to Schlerkmann [21], the main variables that lead to the occurrence and severity of SCC-CO_2 include partial pressure of CO_2, the presence of contaminants, oxygen content, temperature, and its effects on electrolyte characteristics as pH and ionic strength, mechanical and metallurgical properties of the steel and the degree of applied or residual stresses. In general, conditions that favor the non-uniform formation of a passive layer, i.e., its destabilization or local rupture, tend to contribute to localized corrosion and stress corrosion cracking in carbon steels [22].

The corrosion rates depend on several aspects such as the steel grade; the time of exposure to the corrosive environment; the electrolyte dynamics, if it is stagnant or there is a flow speed that influences on mass transport of species due to
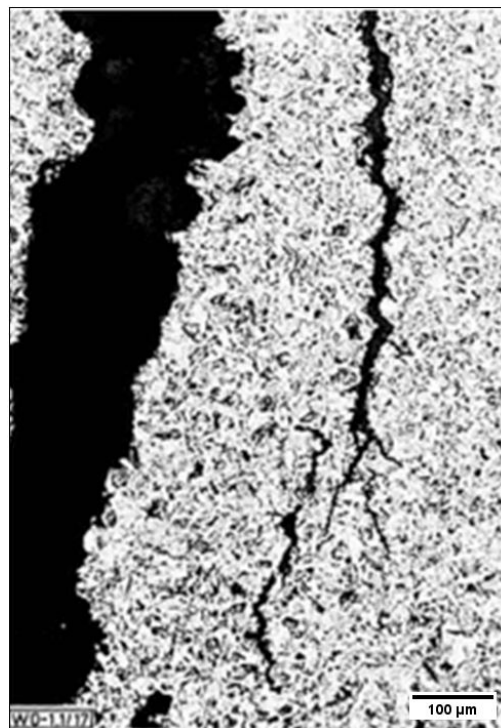

Figure 1. SCC crack from reported cylinders failures by Kunze et al. [13]. *"Reprinted with Permission from John Wiley and Sons".*

shear effects; pressure and temperature of the system; CO_2 partial pressure; salts contents; pH, among others. Corrosion can be reduced if the precipitation rate is in the order of the corrosion rate. If the precipitation is much slower than the dissolution of the steel, the surface will corrode before the protective layer forms. The tendency for the protective layer to form is defined as the ratio between precipitation of iron carbonate and steel corrosion rates. Precipitation occurs when Fe^{2+} and CO_3^{2-} concentrations exceed the solubility product (K_{sp}), which is a function of temperature and ionic strength, while film growth is controlled by crystal growth rate on the steel surface. When this trend exceeds a critical value, defined by Equation 1 [23], the carbonate film begins to form, and corrosion is reduced, depending on the stability of this layer. To achieve noticeable rates of precipitation, supersaturation S should be larger than 1.

$$S = \frac{C_{CO_3^{2-}} \times C_{Fe^{2+}}}{K_{sp}} \tag{1}$$

Corrosion products formed at low temperatures (<40ºC) and low CO_2 partial pressures (<5 bar) tend to be amorphous and show low adherence. Increasing temperature and CO_2 partial pressure show greater crystallinity, good adhesion to the substrate, and protective capacity with consequent lower corrosion rates and high supersaturation values [23,24]. Higher iron concentration in solution also leads to protective $FeCO_3$ film precipitation for pH>5 [23]. Tensile stresses can promote film rupture, collaborating to localized substrate exposition.

4.1 Oxygen presence

When oxygen is present on CO_2/H₂O systems, it can compromise the passiveness of the iron carbonate layer by its dissolution, as the oxides can penetrate deeply through the siderite grain boundaries and finally reach the steel, promoting severe pitting corrosion [25] This fact turns oxygen into an agent that facilitates the exposition of a small anodic area of the substrate to the electrolyte and turns the material susceptible to SCC.

Oxygen also changes the free corrosion potential of iron to positive values in the presence of CO_2, as it gives additional cathodic reaction and consequent increase the corrosion rates. Considering that the crack propagation mechanism is anodic, oxygen can increase the crack propagation rate [26]. Mack´s study regarding CO_2 corrosion of high strength steels shows that complete removal of oxygen from the solution mitigates stress corrosion cracking [27].

4.2 Other contaminants

In the CO_2-H₂O system, the hydrogen generated during corrosion can decrease the time to failure and resistance to cracking. Atomic hydrogen can be embrittling for materials with higher mechanical properties, and CO tends to increase the ingress of hydrogen into the steel by inhibiting its recombination reaction [28]. Carbon monoxide has an inhibiting action on iron dissolution in acidic solutions due to its adsorption capacity on the metal surface. As a result of its electronic structure, CO acts as an adsorption inhibitor, reducing the corrosive process by chemically adsorbing very strongly with the metal. Generalized corrosion is therefore prevented in the presence of CO, and the passive behavior of the surface allows the occurrence of a localized attack assisted by mechanical loading, while the rest of the surface remains inactive [24].

Kowaka and Nagata [29] in the 70s studied the effect of CO and CO_2 contents on SCC of carbon and C-Mn steels through the exposure of "U" bent specimens to aqueous solutions pressurized in a range between 26 and 100 bar. It was found that the higher the partial pressure of CO, the shorter the time to initiate cracks. There was no cracking when the partial pressures of CO and CO_2 were both less than 4 bar in up to 6 weeks of exposure. Cracking occurred at 6 bar of CO_2, and 2 bar of CO. Above about 6 bar CO_2, small amounts of CO can generate cracks. With 16 bar of CO_2, cracks occurred in the samples of carbon steel and C-Mn with min. 0,1 bar of CO. Below this value, no stress corrosion occurred at this CO_2 level. In the absence of CO_2, it appears that cracking occurs at pressures above 10 to 20 bar CO.

Traces of H_2S can considerably increase the corrosion rates of carbon steels. Tang et al. reported that an increase of 59 to 408 ppm H2S strongly accelerates the cathodic reaction of hydrogen evolution, causing severe localized corrosion on carbon steel at 90°C [30]. The effect of H_2S on corrosion of carbon steels consisted of galvanic effects between cementite and pearlite and grain dissolution process. Heterogeneous FeS deposits on the steel surface show low protective characteristics. In this case, the phenomena of SSCC (Sulfide stress corrosion cracking) could be favored. When high corrosion rates form homogeneous film consisting of $FeCO_3$ and FeS, it can be protective and prevent SSCC. H_2S-CO_2 mixtures are complex owing to the numerous elementary conditions which intervene in the failure phenomena in one way or another. One of the significant risks of H_2S corrosion is hydrogen embrittlement and sulfide stress corrosion cracking [30].

4.3 Electrochemical potential and pH

The electrochemical potential has a strong influence on the mechanisms of SCC in CO_2/H₂O systems. The critical range of potentials for SCC occurrence corresponds to the active-passive transition zones as verified by Traversa in the presence of CO [1]. In the pioneering study by Brown et al. [28], it was found that, for CO+CO_2 mixtures in more negative potentials than - 575 mV $_{(SCE)}$, cracks were not observed. Between -575 mV $_{(SCE)}$ and -475 mV$_{(SCE)}$, cracks occurred at progressively higher growth rates in less negative potentials, reaching the maximum crack growth at -475 mV$_{(SCE)}$, above which cracking was replaced by generalized corrosion. Figure 2a combines the dependence of the crack growth

rate as a function of the potential with a polarization curve. The range observed of cracking (-575 and -475 mV $_{(SCE)}$) corresponds to the potential for maximum corrosion inhibition due to CO. There is a reduction of stress corrosion in more anodic potentials, in which inhibition does not occur and generalized corrosion takes place, so according to the authors at potentials more negative than -575 mV $_{(SCE)}$, SCC is minimized due to inhibition of dissolution.

On research from Traversa and Calderón [1] polarization curves of carbon steel samples (0.18% C, 0,65% Mn) were obtained in aqueous solution saturated with CO_2 (pH 5,4) and in another in a mixture containing CO (68%), CO_2 (17%), N_2 (14.4%) and O_2 (0,5%) (pH 6,3). The polarization curves obtained at a scan rate of 2 mV/s for the solutions saturated with CO_2 show the corrosion potential of -685 mV $_{(SCE)}$, while in the presence of CO, it was shifted to -620 mV $_{(SCE)}$. The current densities reduced with the addition of CO: at -1000 mV (SCE), it was respectively 0,06 mA/cm^2 with pure CO_2 and 0,02 mA/cm^2 for the gas mixture. Figure 2b and c show the current density measured in this same study after 24 hours at different applied potentials (together with the polarization curves for comparison). While for CO_2-H_2O system, there is a continuous potentiostatic increase in current with the potential in both potentiodynamic measurements, for CO-CO_2-H_2O solutions, potentiostatic measurements show an increase in current up to -530 mV $_{(SCE)}$, followed by a drop to -500 mV $_{(SCE)}$, and then a new rise was observed. The active-passive transition from -540 to -460 mV $_{(SCE)}$ was identified from these results. This range of susceptibility to SCC-CO_2 is slightly different from the measurement in Brown's et al. study [28], which found this active-passive

transition at 575 and -475 mV $_{(SCE)}$, where maximum crack growth rates were verified (Figure 3).

Grafen and Schlecker [31] have assessed the susceptibility to cracking through slow strain rate tests under electrochemical control on structural steels, with 20 bar CO_2 and 10 bar of CO. It was observed lower loss in ductility for carbon steel at -600 mV $_{(Ag/AgCl)}$. The degradation was more pronounced at more positive and negative potentials from its free corrosion potential. Anodic SCC occurred at active potentials when the passive film shows discontinuity, while for more cathodic potentials, the hydrogen effect was dominant. On research from Krieck et al. [32], the corrosion potential for the three materials was shifted to positive values when increasing partial pressure of CO_2 from 10 to 50 bar at 80°C.

Vancostenable et al. [33] also studied SCC through slow strain rate tests ($\dot{\varepsilon}$ =10^{-7} to 10^{-6} s^{-1}) on smooth and micro-notched samples of a cold-rolled carbon steel (0,3%C) with ferritic-pearlitic elongated microstructure, exposing it to deaerated synthetic seawater saturated with CO_2 with initial pH=6, at OCP and -1200mV $_{(SCE)}$. The smooth samples showed higher elongation to fracture at cathodic potentials compared to OCP. The opposite trend was verified for micro-notched samples, i.e., lower elongation at cathodic potentials. An additional test was performed with a micro-notched specimen deformed at OCP up to 5% of elongation. The potential was changed to cathodic values (-1200 mV $_{(SCE)}$) and kept at this potential until failure. This configuration generated a higher embrittlement level, achieving lower elongation values. The fracture surface showed delamination, ductile tearing, and a brittle cleavage zone. It is believed that the failure mechanism is associated with the formation and growth of microcavities at ferrite/cementite interfaces.
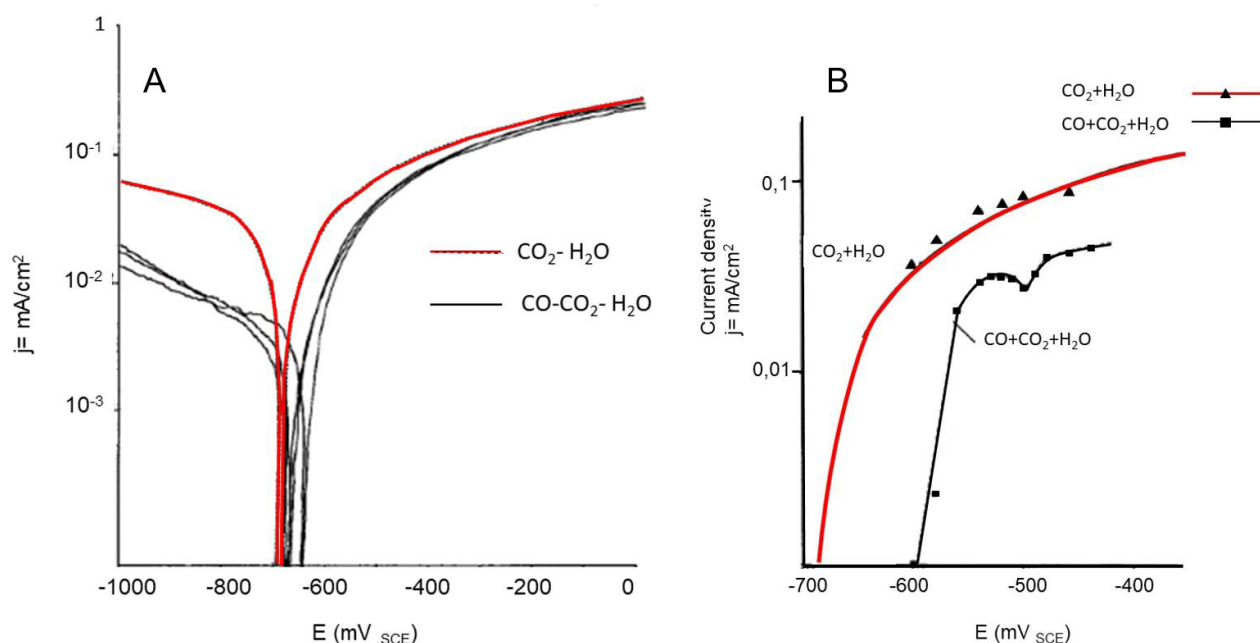

Figure 2. (A) Polarization curves for CO_2/H_2O and CO-CO_2/H_2O systems; (B) Potentiostatic curves at the same system showing active-passive transition at 575 and -475 mV (SCE). Adapted from Traversa and Calderón [1].
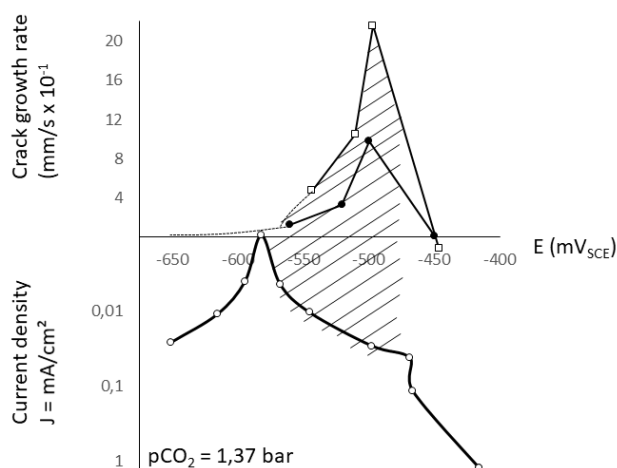
Figure 3. Relation between crack growth rate and extent of CO inhibition as a function of electrochemical potential. Adapted from Brown et al. [28]

Under cathodic polarization, hydrogen is introduced into the material and segregated at these interfaces, promoting embrittlement. In micro-notched samples tested under cathodic potential, a higher concentration of hydrogen occurs at the maximum triaxiality region at the notch tip. At this location, the formation of microcavities and the initiation of cracks were facilitated. At OCP, fractographic analysis suggests that anodic dissolution plays an essential role in crack initiation. The formation of shear bands at the surface generates preferential sites of anodic dissolution. The presence of the notch accelerates the initiation of cracks. There were no signs of dissolution at the crack tip, suggesting that crack propagation was not dominated by anodic dissolution but by hydrogen embrittlement generated by the cathodic reaction associated with the anodic reaction.

The effect of pH can influence SCC´s primary mechanism as its values have implications on SCC potentials [34-36]. The increase in pH tends to reduce the corrosion rates of steel, and the reason is the decrease in hydrogen reduction reaction, lowering the anodic dissolution of steel. Another impact of pH is on the solubility of iron carbonate, which is reduced for higher pH values, leading to the precipitation of a surface layer of $FeCO_3$. The precipitation of siderite occurs at critical pH values dependent on the ionic concentration of Fe_2^+, HCO_3^-, H^+, and the temperature.

Carbon steels are susceptible to high-pH SCC and, according to Parkins and Zhou [11], in solutions containing carbonate and bicarbonate anions at high temperatures. The authors identified that intergranular cracking growth occurred in a narrow range of potentials while transgranular cracks were associated with the severity imposed by high strain level imposed during slow strain rate test. The higher the pH, the higher are HCO_3^- concentrations, and according to Fan et al. [37], the rupture of passive films is promoted by excessive HCO_3^- content, which also facilitates pitting and cracking. Increasing the HCO_3^- concentration increases the

number of defects in the passive film due to the formation of the soluble composite ion $Fe(CO_3)_2^{2-}$ and promotes the anodic dissolution of crack tips [38].

In solutions with near-neutral pH, porous and non-compacted corrosion products are formed, so the passivation of carbon steel does not occur, and this porous structure enables galvanic reactions and hydrogen formation [39]. Inside a crack, this active dissolution produces the crack tip to blunt for static loadings. Another effect that can cause blunt is when the dissolution rates are higher than the strain rate. In this case, the crack generally extends in a 45° direction because of higher shear stresses for plastic deformation. In case of high dissolution rates with a severe attack at the crack tip, this extension cannot be observed once it was consumed by corrosion. Some effects can restart the crack growing at some critical values of K_{max} and ΔK applied in both cases. The hydrogen generated in this near-neutral pH condition must diffuse to the plastic zone ahead of the crack tip to contribute to the crack growth. Chen et al. [40] concluded that crack growth in a near-neutral pH environment is a competitive process at the crack tip, between intrinsic blunting and extrinsic sharpening. The former is due to active dissolution during near-static loads or low-frequency cyclic loads over the deformed crack tip without passivation of its surface, while extrinsic sharpening is governed by fatigue and hydrogen embrittlement. For static loadings, the cracks remain dormant. When cyclic loads were applied, the blunting process was attenuated by the sharpening process. So, the balance of both process determines whether cracks will grow actively or will remain dormant.

4.4 Temperature

The temperature effect is quite complex once it affects the ion concentration at the electrolyte, consequently changing the pH and electrode potential. On Schmitt/Schlerkmann papers [41], the anomalous behavior of 37Mn5 steel might be related to a larger pit density found at both 40ºC and 60ºC, although 40ºC seemed to be more severe. However, we ought not to take this as universal as the behavior depends on factors such as inclusion type/density, CO_2 partial pressure [22], and the applied potential [11]. The cracks in 37Mn5 steel samples that showed premature fracture (40ºC, 60 bar) are predominantly wide, blunt, and show a branched appearance, with some fine and deep cracks. Few pits were seen at this temperature. The cracks identified in those samples were more profound than those tested at 60 bar and 25ºC, where a higher number of cracks but deepest were observed. At 25ºC, many cracks grew from corrosion pits and showed sharper morphologies. Cracks and pits identified occurred in general along the lines of MnS inclusions. There were no cracks in samples tested at 60 bar / 60ºC, the only evidence of crack initiation at the bottom of corrosion pits.

In the scope of Van der Merwe´s [24] thesis, fracture mechanics tests using double cantilever beam (DCB) specimens from C-Mn plate steel were performed in CO-CO_2 solutions,

varying the temperature and O_2 content. For the most critical condition, with 8 ppm of oxygen, the threshold values for crack propagation (K_{ISCC}) were 5 MPa.m$^{1/2}$ at 25ºC and 7 MPa.m$^{1/2}$ at 45ºC. With 0.1 ppm O2, K_{ISCC} was 20 MPa. m$^{1/2}$ at 25ºC and 15 MPa. m$^{1/2}$ at 45ºC. At 25ºC, crack growth rate (da/dt) varied between $1-2.10^{-11}$ m / s (0.3-0.6 mm/ yr), while at 45ºC, it varied between $3-7.10^{-10}$ m/s (9.5 to 22 mm/yr). Crack growth rates were more affected by temperature, not being decisively altered by the oxygen content.

In more recent studies conducted by Schmitt, it was found that no temperature effect was observed for 10 bar of CO_2, only at 60 bar [41].

4.5 Metallurgical aspects that influence SCC

Materials-related parameters such as chemical composition, microstructure orientation, distribution of precipitates and inclusions, dislocation interactions, and progress of the phase transformation (or degree of metastability) and consequent properties as hardness and tensile strength can affect SCC susceptibility. It is well known that higher mechanical strength materials show more susceptibility to SCC. There are limitations to certain materials regarding their hardness when exposed to determined sulfur-containing environments [42]. As verified in Schlerkmann´s thesis [21], in general, greater susceptibility to SCC-CO_2 occurs in conditions where materials are more prone to pitting. In this sense, molybdenum additions may be a potential parameter to increase the resistance to this cracking phenomenon.

Critical values of the tendency to form the carbonate layer for effective protection are presented for different microstructures and carbon content for mild steels in Van Hunnik´s study. It is known that carbon steels with more than 0.15% C can form a cementite/carbide network that remains after corrosion of ferrite. This network increases the local supersaturation level, resulting in forming a protective film in smaller supersaturations. Furthermore, cementite can significantly affect the residual current through the film and its protection capacity [43,44]. In the case of mild steels, when a solution is present, galvanic effects between carbon-rich structures and ferrite grains induce micro-cracks. In the case of pearlitic-ferritic steels, cementite acts as a cathode due to a lower overpotential for hydrogen evolution, and ferrite as an anode resulting in the preferential attack, as verified by Lopez e Al Hassan in CO_2 environments [27,45,46].

The minimum content of 9% Cr was shown to be necessary to prevent cracking. Steels containing high Cr content such as corrosion-resistant alloys have good resistance to pitting corrosion due to the high Cr content in corrosion products´ surface layer. They can, however, become susceptible to pitting in the presence of chlorides and oxygen. Baéz and Vera [47] measured the critical pitting temperatures using Electrochemical Noise at high pressures of 13Cr, super 13Cr, and 22Cr in solutions with 1 and 10% NaCl and 41 bar CO_2. The 13Cr alloy had the worst performance, with a CPT of 105ºC, while the other two materials showed critical pitting temperature (CPT) above the maximum test temperature (166ºC).

The surface finish of steels also affects SCC resistance in CO_2 environments. Stress corrosion cracks can nucleate at machining marks or scratches, or material with high roughness values tend to increase SCC susceptibility. Kowaka and Nagata [48] demonstrated that more severe cracking was observed in samples with oxides that originated during the rolling process (the occurrence of cracks at 30% YS) than with samples surface finished by grinding, where cracks occurred at 50% YS.

4.6 Applied and residual stresses

Applied or residual stresses should be considered when environmentally evaluating assisted cracking. One of the three pillars to SCC-CO_2 occurrence is the stress field distribution on the material. These are composed of different sources: the residual and the applied stresses. The former is originated during material processing and is typically not uniformly distributed. The latter is a consequence of applied external loads and generally has a well knows distribution. The total stress on the material will be the arithmetic sum of both residual and applied stress. The SCC nucleation occurs below the material yield strength of the bulk material and typically below the design stress or fatigue limit [49].

The tensile stress is mostly resulting from static load conditions, those global stresses are below the macroscopic yield limit (linear elastic-region), but locally they reach a higher value due to stress intensification. When this reaches a value higher than a threshold value, it will cause a localized and microscopic (material grain size order) yield. This understanding is based on the passive film breakage theory assisted by a dislocation movement towards the stress concentration regions (e.g., crack tip) [50]. The dislocation movement in those specific paths follows the maximum local stress and is one of the conditions to promote SCC.

Although stress is an essential parameter on SCC, there is little research focused on defining the role of stresses in crack initiation and growth. In an investigation by Beavers et al., they found a valid empirical correlation between residual stress and SCC incidence [51]. Boven et al. [49] found the formation of micro-pitting to a depth of up 200μm occurred in areas where tensile residual stresses of 300 MPa and SCC nucleated at the bottom of the pits. They also concluded that for long-term tests, the crack growth rate increased with increasing residual stresses, while for short term tests, there is a residual stress threshold value for crack initiation.

Leading to SCC on high strength steel wires, test results demonstrated a power inverse relation between the tensile stresses and the average life of susceptible materials in the same aggressive environment [52], showing the stress dependency on time to failure for a high strength steel in a test solution containing: 0,45g/l of NaCl, 1,5 g/l NaS, 0,9 g/l $CaSO_4$, 25 g/l of Acetic Acid, the solution pH was 2,4.

The presence of high tensile residual stress below the surface influences the formation of crack colonies. As the residual stress distribution is not uniform, the colony location dependency can be explained once the same environment cannot produce colonies, and one crack inside a colony can be short or long, depending on the residual stress distribution in the steel´s depth direction [53,54].
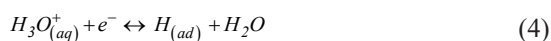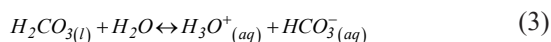
4.7 Hydrostatic pressure

A lack of information regarding the effect of higher hydrostatic pressure on corrosion cracking could be found in the literature. Hydrostatic pressure (HP) can lead to a sudden increase in mechanical driving force on a component containing a microcrack and inducing a restart of propagation after a crack tip blunting in case of crack dormancy or a microcrack previously nucleated at corrosion pits [55].

Yang et al. assessed the normalized stress with crack time in a range of hydrostatic pressures. The normalized stress decreases with increasing hydrostatic pressure, which indicates that SCC can be promoted by hydrostatic pressure. To prove the possible relation between SCC susceptibility and hydrostatic pressure, they showed the plastic loss increased proportionately with hydrostatic pressure, which means the HP assisted the SCC susceptibility of X70 pipeline steel. During electrochemical tests, the potentiodynamic polarization curves clarify that a higher hydrostatic pressure facilitates the cathodic reaction demonstrated by the increase in cathodic Tafel slopes (βc), and the corrosion process, where the corrosion potential and corrosion current density increase with hydrostatic pressure. The diffusible hydrogen measured on samples by hot extraction after 200h of immersion shows a pressure dependency, as shown in Figure 4 [56].
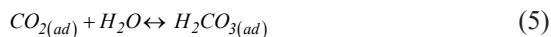
5 SCC mechanisms

The environment surrounding a metal during corrosion plays a vital role in the nucleation and propagation of stress corrosion cracks. SCC-CO_2 depends on corrosion and passivation rates, so it is dependent on CO_2 corrosion mechanisms. In deoxygenated solutions containing CO_2 at ambient temperature, the corrosion rate of a carbon steel is controlled by hydrogen evolution kinetics and can be described by the following reactions, proposed by Schmitt [57]. According to his study, the hydrogen evolution occurs following two different steps. The first postulate that dissolved CO_2 hydrate at the bulk of solution forming carbonic acid H_2CO_3 (Equation 2). The acid can dissociate from the bulk and migrate to the steel surface. During this dissociation reaction (Equation 3), $H3O^+$ ions will form and reduce electrochemically, liberating hydrogen that will adsorb on the steel surface (Equation 4).

$$CO_{2(d)} + H_2O \leftrightarrow H_2CO_{3(l)} \tag{2}$$

$$H_2CO_{3(l)} + H_2O \leftrightarrow H_3O^+_{(aq)} + HCO_3^-_{(aq)} \tag{3}$$

$$H_3O^+_{(aq)} + e^- \leftrightarrow H_{(ad)} + H_2O \tag{4}$$

Another sequence suggests that hydrogen release occurs by the hydration of CO_2 as a heterogeneous reaction directly on the steel surface, Equation 5, where the acid can be reduced directly or dissociate, generating ions H_3O^- (Equation 6) that will reduce and generate H^+ as described by This study suggests that the controlling step is the heterogeneous hydration of CO_2 at the steel surface. Bicarbonate anions will react with iron cations at the steel surface, forming iron carbonate ($FeCO_3$) as a corrosion product (Equation 7).

$$CO_{2(ad)} + H_2O \leftrightarrow H_2CO_{3(ad)} \tag{5}$$

$$H_2CO_{3(ad)} + e^- \leftrightarrow H^+_{(ad)} + HCO_3^-_{(ad)} \tag{6}$$

$$Fe^{2+} + HCO_3^- \leftrightarrow FeCO_{3(s)} \tag{7}$$

Several mechanisms have been proposed to explain the synergy between stresses, environment, and susceptible materials to SCC but is not well defined or wholly supported by scientific studies to date. Some of those mechanisms are the adsorption model, pre-existing active path model, film
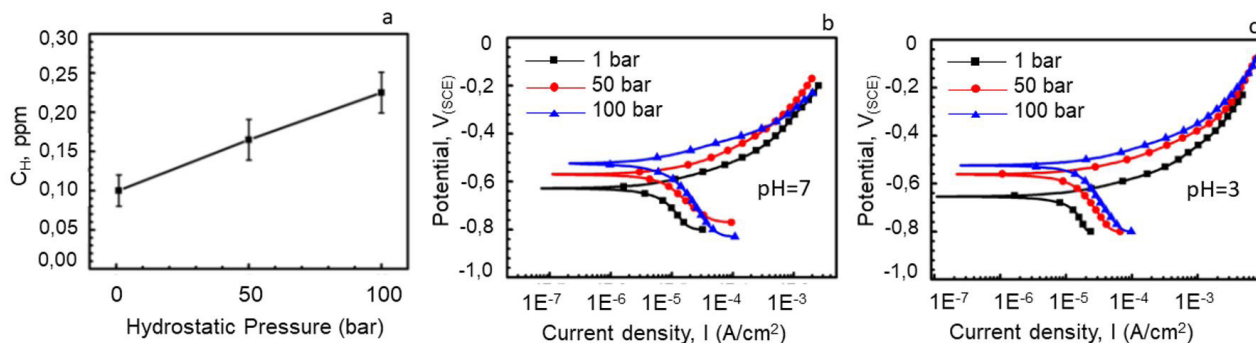

Figure 4. (a) Diffusible hydrogen concentration in steel vs hydrostatic pressure after 200h immersion test; potentiodynamic polarization curves at (b) pH=7 and (c) pH=3. Adapted from Yan et al. [56].

rupture model, and hydrogen embrittlement (HE). Among them, mechanisms based on the anodic dissolution of new metal created by slip bands at the crack tip are often regarded as the most reliable model [58-61].

There is no consensus on the mechanisms since the combination of the parameters involved can be quite complex. Furthermore, both dissolution and hydrogen evolution can co-occur under appropriate circumstances [62].

According to Lynch [60], the main atomistic processes that occur at the crack tip leading to crack growth are: (a) the removal of metallic atoms from the crack tip to the surrounding environment; (b) shear movement of atoms at crack tips generating the emission or egress of dislocations; (c) decohesion of atoms by tensile stress that can involve shear movements between atoms and (d) surface diffusion of atoms from the crack tip to adjacent locations. Based on these processes, some mechanisms have been proposed for SCC and hydrogen embrittlement (HE). The characteristics of fracture surfaces produced by SCC and (HE) are often similar, differing in the characteristics of the corrosion films, since SCC dissolution occurs and for HE, it does not. So, the hydrogen-based SCC mechanisms are essentially the same as those proposed for HE. Moreover, they involve so much adsorbed hydrogen, dissolved hydrogen, or hydrides at the crack tips. Comparing SCC involving hydrogen and Hydrogen embrittlement, there are subtle differences [61].

Mechanisms based on anodic dissolution involve removing atoms just in front of the crack tip, preferably in a direction normal to the applied or residual stress. Dissolution can be promoted by active paths that can be chemically active, such as grain boundaries or steps generated by stress or strain fields in front of the crack tip, and dissolution can be limited by forming a passive film on the fracture surface. The slip-dissolution mechanism is the most mentioned dissolution-based mechanism in the literature, which involves breaking passive films by slip bands that intersect the crack tip, promoting dissolution. The crack tip may have a film-free appearance if the strain rate is higher than the repassivation rate [11,58,59].

In those cases where the fracture occurs easily at cathodic potentials, the process that defines fracture is hydrogen embrittlement, once the situation permits that hydrogen can be formed [62] For anodic zones where the proposed mechanisms involve dissolution, hydrogen can be generated at the front of the corrosion layer (for example, at the bottom of pits) and spreads to the adjacent unaffected material establishing a hydrogen diffusion zone. Therefore, even in the anodic zone is possible to get hydrogen embrittlement [63]. So, materials that suffer embrittlement in the cathodic zone can also be tested at the anodic zone to verify the possibility of fragilization started from corrosion pits. Figure 5 schematically resumes the corrosion mechanisms distributed along the corrosion potentials according to literature data [11,58-62].

SCC mechanisms from a crack path point of view can be divided into intergranular (I) and transgranular (T). I-SCC cracks initiate and propagate along the material´s grain boundaries, as they contain more structural defects and sites for impurities, improving selective anodic dissolution that can be further promoted by grain boundary slip. Currently, a consensus exists that in most cases, I-SCC takes place under a preferential dissolution mechanism. On the other hand, T-SCC is believed to occur by environmentally induced cleavage, but the way the environment produces cleavage is not well understood. Several mechanisms have been proposed to explain this type of embrittlement, but they all do not have a broad acceptance [60,61].
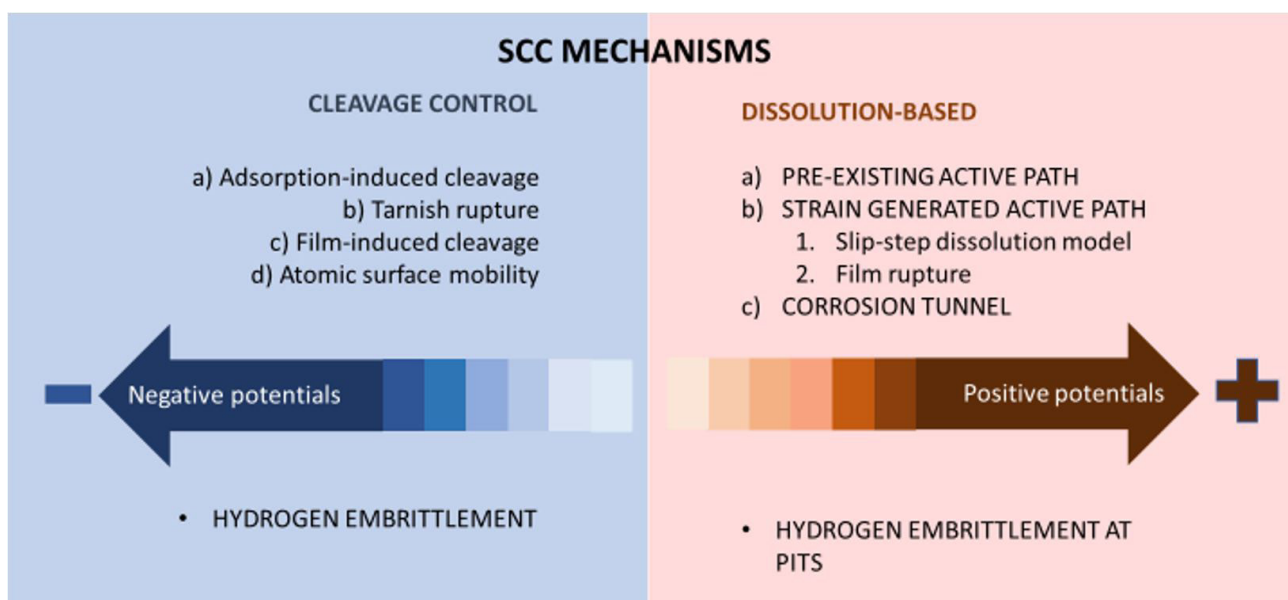

Figure 5. Resume of stress corrosion cracking mechanisms [11,58-62].

6 Susceptibility to cracking evaluation

To determine the susceptibility of alloys to SCC, several types of tests are available, and the right choice comes from the specialist to determine the objective of the testing. If the objective is to predict service behavior or to select alloys for service in a specific condition, it is often necessary to find SCC information in a relatively short time, that requires acceleration of testing. This can be achieved by increasing the severity of the environment, or some critical parameters, such as temperature, pressure, the concentration of species, presence of contaminants, and electrochemical stimulation. Stress-corrosion specimens can be divided into two categories: smooth and pre-cracked or notched. Further distinctions can be made in the loading mode, such as monotonic rising loads, cyclic or ripple loads, constant deflection, constant load, and strain rate [64,65].

Time to failure data obtained by constant load or constant strain tests in a determined environment usually require longer times of exposure. A constant load test generally results in a graph of the stress applied against total time to failure. This graph allows to obtain the threshold stress (σ_{TH}), below which there will be no failure by environment assisted cracking. For practical purposes, the test is complete after a pre-specified time. In this case, the presence or the number of cracks is used as a criterion for failure or susceptibility. Constant displacement tests such as C-ring, U-ring, bent beam, and four-point bending are also extensively used. Sample preparation and some recommendations are found in standards ASTM G49 [66], ASTM G39 [67], NACE TM 0177 (NACE-TM-0177, 2016) [68], and ISO 7539 part 2 to 5 [69].

Slow strain rate tests (SSRT) the test specimen is subjected to a constant and low strain rate, preferentially lower than 10^{-6} s^{-1} [70] to give time for the environment to interact with the material while exposed. The inconvenience of this test is the excessive strain imposed at test samples, sometimes leading to cracking at strains greater than those applied during component service. The results of this test are presented comparing the performance in the environment with the air. The main normative reference for this test is ASTM G129 [71]. One variation of SSRT is incrementally applying displacement or load, or step loading, whose recommendations are described in standard ASTM F1624 [72].

Pre cracked samples consider fracture mechanics concepts and are applied to characterize the initiation and growth of cracks from these pre-existing flaws. It can be used to determine underdetermined environmental conditions, the material fracture toughness, threshold values for crack growth, and predict crack growth rates. This information can be used even for materials selection and structural integrity assessment, considering the damage tolerance philosophy [73].

Stress corrosion tests using potentiostatic or potentiodynamic polarization provide the domains of immunity, general corrosion, passivation, and pitting for a determined metal-environment system Through the acquisition and interpretation of some characteristic potentials such as corrosion potential, primary passivation potential, breakdown potential and protection potential. Those parameters can provide a good correlation between SCC susceptibility and the electrochemical behavior of the alloy/environment system. From this, a better understanding of the mechanism of SCC can be obtained [64].

In a study by Hudgins et al. [2] on C-Mn samples using method C from NACE TM0177 [68], samples with a machined notch were constant loaded between 20 and 130% of material's yield strength and then exposed to a deoxygenated NaCl 5% solution, pressurized with CO₂ at 1 and 20 bar, all in stagnant conditions, that is, no gas replenishment. Early failures occurred only for high strength steels (33-34 HRC) at 20 bar and higher loading conditions (115% YS). They found that 20 bar was sufficient to crack initiation in a highly stressed and high resistance carbon steel alloy after 13 days of exposure [74]. In this study, only high strength steels showed premature failures. Other materials tested with lower properties did not fail.

Schlerkmann [21] is one of the main references regarding stress corrosion cracking on CO₂/H₂O system. Three different materials employed on CO₂ cylinders (C-Mn and C-Cr steels) were evaluated in this study, and each one heat-treated to obtain different mechanical properties. Cylindric samples were loaded at 50% and 90%YS and exposed to brine solution for 42 days, and pressurized at 10 and 60 bar of CO₂, at temperatures between 0 and 60ºC. The relation of solution volume to free steel area is 10,3 mL/cm². In this study, Schlerkmann observed a tendency for cracking with increasing CO₂ pressure, temperature, mechanical properties, and applied loads. Fractures occurred on materials with YS higher than 700 MPa and CO₂ pressures above 10 bar, but cracks were found at 25°C and 50% YS. Figure 6 resumes the results at 60 bar, showing, in contrast, the condition that results in total failure. Comparing the incidence of pits and cracks, it appears that, in general, greater susceptibility to SCC occurs under conditions that are more prone to pitting. This is plausible since both local corrosion and SCC tend to favor low stability conditions of the protective layers. Also, the depth of the cracks and pits formed has decreased with the decrease in stress levels.

For 37Mn5 steel, premature failures occurred on high strength samples at 60 bar and 40°C. At the same pressure at 25°C, this grade has failed after 1000h at 96%YS. Those were the faster failures between all steels and grades tested. The relative values of reduction in area for fracture for 37Mn5 are shown in Figure 7 as a function of temperature for 10 and 60 bar of CO₂. In general, significant susceptibility to failure occurs for higher mechanical strength materials and higher CO₂ partial pressures. It was verified under 60 bar of CO₂ that, in general, the most significant susceptibility (less reduction of the relative area, that is, greater embrittlement) occurs at intermediate temperatures, that is, at 40 and 25ºC. At 60ºC, the embrittlement is very small concerning the values obtained in the air. It is concluded that this steel has low susceptibility to stress corrosion at higher temperatures. The
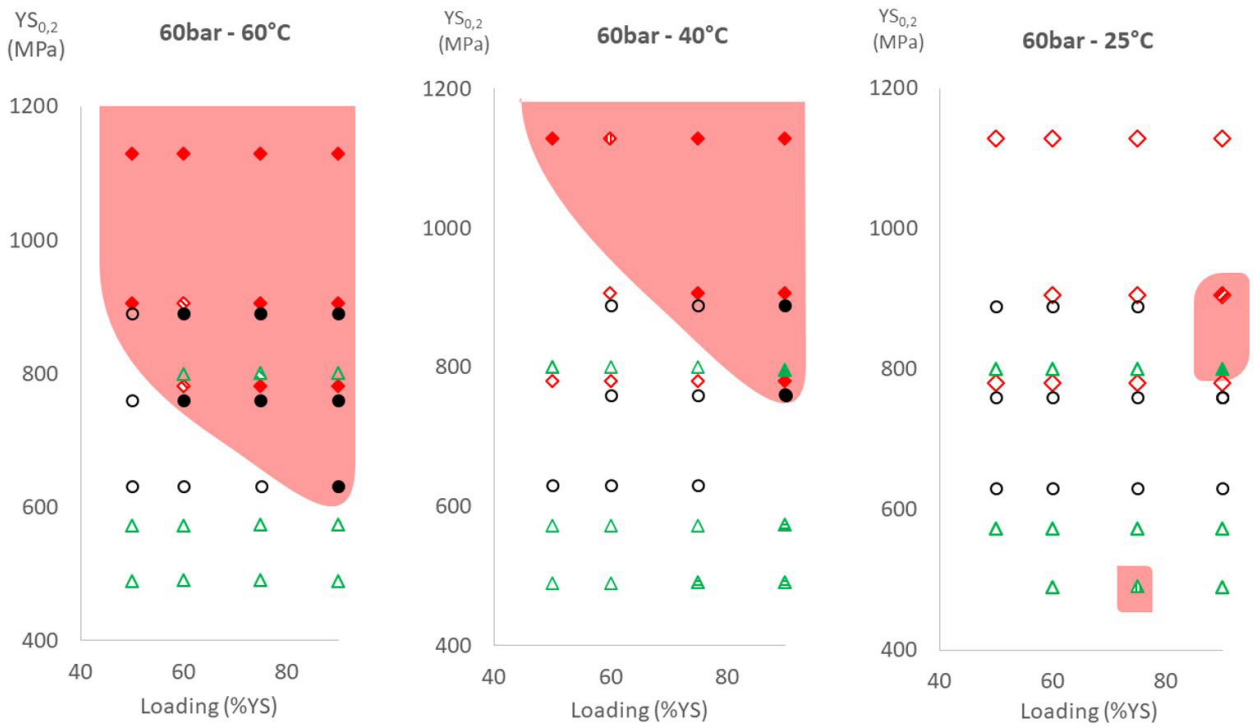
Figure 6. Occurrence of SCC on CO_2/H_2O system at 60 bar. ♦30CrNiMo8; ●34CrMo4; ▲37Mn5. Filled symbols: cracks; semi-filled symbols: cracks initiation; empty symbols: no cracks. Adapted from Schlerkmann [21].
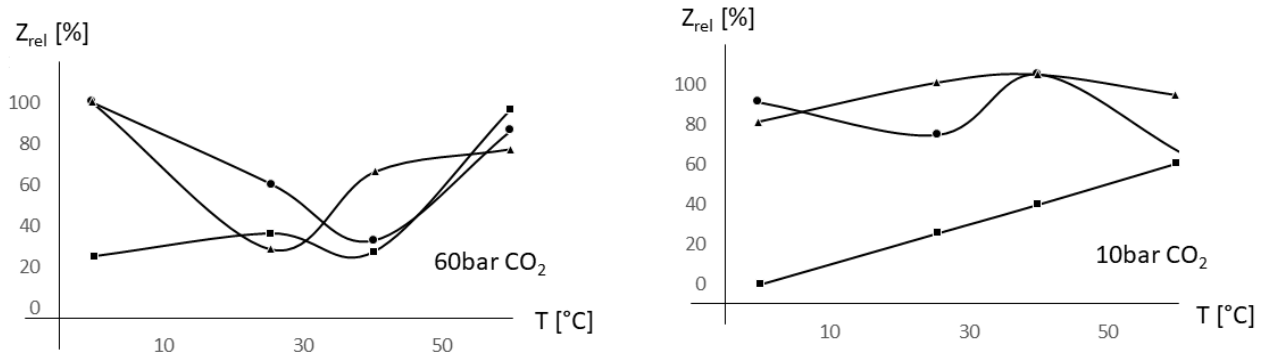

Figure 7. Effects of Temperature and CO_2 pressure on reducing the area for fracture at 90%YS for steel 37Mn5. Mechanical properties levels: ■: A (YS 490 MPa); •: B (YS 578 MPa); ▲: C (YS 795 MPa). Adapted from [21].
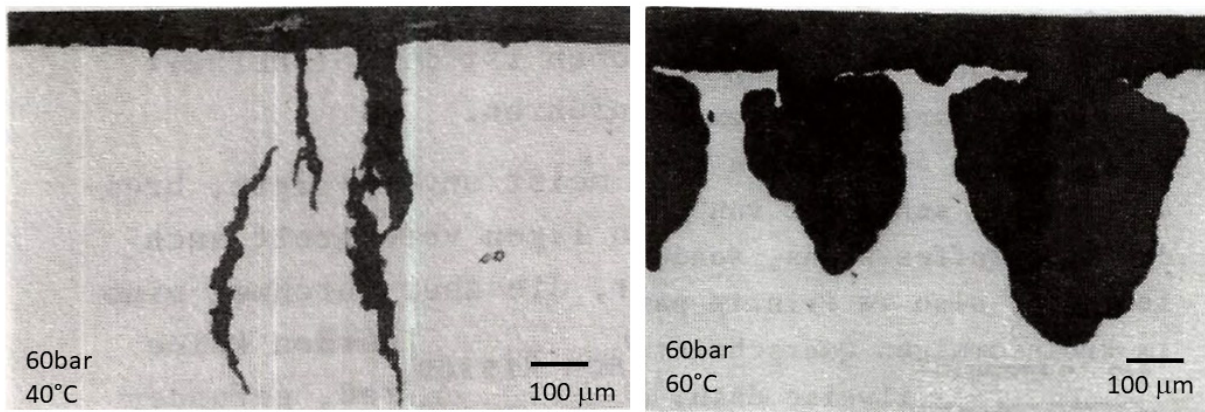

Figure 8. Morphology of a crack formed at 40°C (left) and corrosion pits formed at 60°C (right), both at 60 bar CO2 for 37Mn5 steel. Adapted from Schlerkmann's RWTH Thesis [21].

cracks identified in the sample tested at 60 bar / 40ºC were deeper, while the sample tested at 60 bar / 25ºC showed a higher number of cracks but less deep. At 25ºC, many cracks grew from corrosion pits (Figure 8). At 0ºC, for the harder steel, the formed pits acted strongly in reducing ductility. Under 10 bar of CO_2, few conclusive trends have been seen.

7 Conclusions

According to the stress corrosion mechanisms based on dissolution through film rupture, a superficial layer of corrosion products is a condition for the SCC occurrence by CO_2 in carbon steel, C-Mn, and low alloys steels. Localized destabilization of this layer by local dissolution assisted by ions or oxygen, strain or cracking of this film, or other processes can generate localized corrosion on a steel substrate. Crack propagation occurs in conditions where there is no precipitation of corrosion products at the crack tip. For SCC, the prediction of crack growth rate is still a challenging subject because of the complex nature of the synergistic interactions among the environment, the material, and the stress that involve electrochemical and mechanical processes.

Additional evidence suggests that hydrogen-assisted crack growth appears to be an essential part of the phenomenon´s mechanism once there is an intense generation of hydrogen in CO_2 corrosion. Some parameters that favor the occurrence of SCC of carbon steels in the presence of CO_2 are partial pressures of CO_2, steels with high mechanical properties, presence of contaminants such H2S, CO, and O_2, high-stress levels (applied or residual), and presence of plastic strain.

The occurrence of pitting is associated with the formation of cracks. In this way, it is possible that, in the conditions of short tests in which pits were found, cracks occur under longer times and slightly more aggressive conditions.

Acknowledgements

References

1   Traversa E, Calderón T. Electrochemical investigation on carbon steel behaviour in CO-CO2-H2O environment for the interpretation of the SCC mechanism. Werkstoffe und Korrosion. 1991;42(1):35-40. http://dx.doi.org/10.1002/maco.19910420106.

2   Hudgins C, McGlasson R, Mehdizadeh P, Rosborough WM. Hydrogen sulfide cracking of carbon and alloy steels. Corrosion. 1966;1966(8):238-251. http://dx.doi.org/10.5006/0010-9312-22.8.238.

3   Barker R, Burkle D, Charpentier T, Thompson H, Neville A. A review of iron carbonate (FeCO3) formation in the oil and gas industry. Corrosion Science. 2018;142:312-341. http://dx.doi.org/10.1016/j.corsci.2018.07.021.

4   Motte R, Basilico E, Mingant R, Kittel J, Ropital F, Combrade P, et al. A study by electrochemical impedance spectroscopy and surface analysis of corrosion product layers formed during CO2 corrosion of low alloy steel. Corrosion Science. 2020;172:108666. http://dx.doi.org/10.1016/j.corsci.2020.108666.

5   Gao K, Yu F, Pang X, Zhang G, Qiao L, Chu W, et al. Mechanical properties of CO2 corrosion product scales and their relationship to corrosion rates. Corrosion Science. 2008;50(10):2796-2803. http://dx.doi.org/10.1016/j.corsci.2008.07.016.

6   Dai H, Shi S, Guo C, Chen X. Pits formation and stress corrosion cracking behavior of Q345R in hydrofluoric acid. Corrosion Science. 2020;166:108443. http://dx.doi.org/10.1016/j.corsci.2020.108443.

7   Mai W, Soghrati S. A phase field model for simulating the stress corrosion cracking initiated from corrosion pit. Corrosion Science. 2017;125:87-98. http://dx.doi.org/10.1016/j.corsci.2017.06.006.

8   Wang W, Zhou A, Fu G, Li C, Robert D, Mahmoodian M. Evaluation of stress intensity factor for cast iron pipes with sharp corrosion pits. Engineering Failure Analysis. 2017;81:254-269. http://dx.doi.org/10.1016/j.engfailanal.2017.06.026.

9   Rogowska M, Gudme J, Rubin A, Pantleon K, Ambat R. Effect of Fe ion concentration on corrosion of carbon steel in CO2 environment. Corrosion Engineering, Science and Technology. 2016

10   Rosli N. The effect of oxygen in sweet corrosion of carbon steel for enhanced oil recovery [dissertation]. Athens, OH: Russ College of Engineering and Technology; 2015.

11   Parkins RN, Zhou S. The stress corrosion cracking of C-Mn steel in CO2-HCO3-, CO32- solutions. I: stress corrosion data. Corrosion Science. 1997;39(1):159-173. http://dx.doi.org/10.1016/S0010-938X(96)00116-3.

12   Rhodes P. Stress cracking in corrosive oil and gas wells. Houston, Texas: NACE Corrosion; 1986.

13   Kunze, E., Gerken, G., Nowak, J. Ergebnisse des Forschungs und Entwicklungsprogramms "Korrosion und Korrosionsschutz". Werkstoff und Korrosion. 1979;30:809-811.

14 Spähn, H., Wagner, G., Steinhoff. Betriebliche und sicherheitstechnische Aspekte der Spannungsrisskorrosion. Technische Überwachung; 1973. p. 260-264.

15 Wendler-Kalsch, E., Gräfen, H. Korrosionsschadenkunde. USA: Springer-Verlag; 2012.

16 Sadeghi Meresht E, Shahrabi Farahani T, Neshati J. Failure analysis of stress corrosion cracking occurred in a gastransmission steel pipeline. Engineering Failure Analysis. 2011;18(3):963-970. http://dx.doi.org/10.1016/j.engfailanal.2010.11.014.

17 Manfredi C, Otegui JL. Failures by SCC in buried pipelines. Engineering Failure Analysis. 2002;9(5):495-509. http://dx.doi.org/10.1016/S1350-6307(01)00032-2.

18 Wang J, Atrens A. Analysis of service stress corrosion cracking in a natural gastransmission pipeline, active or dormant? Engineering Failure Analysis. 2004;11(1):3-18. http://dx.doi.org/10.1016/j.engfailanal.2003.08.001.

19 Hasan F, Iqbal J, Ahmed F. Stress corrosion failure of high-pressure gas pipeline. Engineering Failure Analysis. 2007;14(5):801-809. http://dx.doi.org/10.1016/j.engfailanal.2006.11.002.

20 Abedi S, Abdolmaleki A, Adibi N. Failure analysis of SCC and SRB induced cracking of a transmission oil products pipeline. Engineering Failure Analysis. 2007;14(1):250-261. http://dx.doi.org/10.1016/j.engfailanal.2005.07.024.

21 Schlerkmann, H. Zur Frage der rissbildenden Korrosion von niedriglegierten Vergütungsstählen im System CO_2/H_2O. [thesis]. Aachen: RWTH Aachen University, 1982.

22 Schmitt G, Hörstemeier M. Fundamental aspects of CO_2 metal loss corrosion – Part II: influence of different parameters on CO_2 corrosion mechanisms. Corrosion. 2006. Paper presented at the CORROSION 2006, San Diego, California, March 2006.

23 Nešić S, Nordsveen M, Nyborg R, Stangeland A. A mechanistic model for carbon dioxide corrosion of mild steel in the presence of protective iron carbonate films—Part 2: a numerical experiment. Corrosion Science. 2003;59(6):489-497.

24 Van der Merwe J. The stress-corrosion cracking of carbon steel in CO-CO_2-H_2O [thesis]. Pretoria: University of Pretoria; 2013.

25 Rosli N, Choi Y, Young D. Impact of oxygen ingress in CO_2 corrosion of mild steel. Corrosion. 2014. Paper presented at the CORROSION 2014, San Antonio, Texas, USA, March 2014.

26 Dugstad A, Morland B, Clausen S. Corrosion of transport pipelines for CO_2 – effect of water ingress. Energy Procedia. 2011;4:3063-3070. http://dx.doi.org/10.1016/j.egypro.2011.02.218.

27 Mack R. Stress corrosion cracking of high strength steels in aqueous solutions containing CO_2 - Effects of Yield Strength, Dissolved Oxygen, and Temperature. Corrosion. 2001. Paper presented at the CORROSION 2001, Houston, Texas, March 2001.

28 Brown A, Harrison J, Wilkins R. Electrochemical investigation of stress corrosion cracking of plain carbon steel in the CO-$CO2$-$H2O$ system. In: National Association of Corrosion Engineers – NACE. International Conference on Stress Corrosion Cracking and Hydrogen Embrittlement of Iron Base Alloys; 1973; Unieux-Firminy, França. Houston, Texas: NACE; 1973.

29 Kowaka M, Nagata S. Stress Corrosion Cracking of mild and low steels in $CO2$-CO-$H2O$ environments. Corrosion. 1976. http://dx.doi.org/10.5006/0010-9312-32.10.395.

30 Tang J, Shao Y, Guo J, Zhang T, Meng G, Wang F. The effect of $H2S$ concentration on the corrosion behavior of carbon steel at 90 C. Corrosion Science. 2010;52(6):2050-2058. http://dx.doi.org/10.1016/j.corsci.2010.02.004.

31 Gräfen, H., Schlecker, H. Rissschäden an unlegierten Stählen in CO-$CO2$-$H2O$-Gemischen durch anodische oder wasserstoffinduzierte Spannungsrisskorrosion ausgelöst? Aufklärung des Mechanismus und Festlegung von Schutzmassnahmen. Werkstoffe und Korrosion. 1984;35:273-310.

32 Krieck-Defrain, M. Zum- Einfluß von Medien- und Werkstoffparametern auf die Metallauflösung, Wasserstoffaufnahme und Deckschichteigenschaften bei der Stahlkorrosion unter erhöhten $CO2$-Drücken. [thesis]. Aachen: RWTH Aachen University, 1989.

33 Vancostenoble A, Duret-Thual C, Bosch C, Delafosse D. Stress corrosion cracking of ferrito-pearlitic steel in aqueous environment containing dissolved $CO2$. Corrosion. 2014. Paper presented at the CORROSION 2014, San Antonio, Texas, USA, March 2014.

34 Wang S, Lamborn L, Chevil K, Gamboa E, Chen W. On the formation of stress corrosion crack colonies with different crack population. Corrosion Science. 2020;168:108592.

35 Javidi M, Horeh S. Bahalaou. Investigating the mechanism of stress corrosion cracking in near-neutral and high pH environments for API 5L X52 steel. Corrosion Science. 2014;80:213-220. http://dx.doi.org/10.1016/j.corsci.2013.11.031.

36 Lu BT, Song F, Gao M, Elboujdaini M. Crack growth model for pipelines exposed to concentrated carbonate-bicarbonate solution with high pH. Corrosion Science. 2010;52(12):4064-4072. http://dx.doi.org/10.1016/j.corsci.2010.08.023.

37 Fan L, Du C, Liu Z, Li X. Stress corrosion cracking of X80 pipeline steel exposed to high pH solutions with different concentrations of bicarbonate. International Journal of Minerals Metallurgy and Materials. 2013;20(7):645-652. http://dx.doi.org/10.1007/s12613-013-0778-4.

38 Burstein DH, Burstein GT. The effects of bicarbonate on the corrosion and passivation of iron. Corrosion. 1980

39 Meng GZ, Zhang C, Cheng YF. Effects of corrosion product deposit on the subsequent cathodic and anodic reactions of X-70 steel in near-neutral pH solution. Corrosion Science. 2008;50(11):3116-3122. http://dx.doi.org/10.1016/j.corsci.2008.08.026.

40 Chen W, Kania R, Worthingham R, Boven GV. Transgranular crack growth in the pipeline steels exposed to near-neutral pH soil aqueous solutions: the role of hydrogen. Acta Materialia. 2009;57(20):6200-6214. http://dx.doi.org/10.1016/j.actamat.2009.08.047.

41 Schmitt, G, Sobbe,L.,Bruckoff, W. Corrosion and hydrogen-induced cracking of pipeline steel in moist triethylene glycol diluted with liquid hydrogen sulfide. Corrosion Science, 1987; 27(1071-1076).

42 American National Standards Institute. NACE-MR0175. Petroleum And Natural Gas Industries - Materials For Use In H2S-Containing Environments In Oil And Gas Production (includes parts 1, 2, and 3). Washington: ANSI; 2015.

43 Remita E. Étude de la corrosion d'un Acier faiblement allié en Mileu confiné contenant du CO2 dissous [thesis]. Paris: Université Pierre et Marie Curie; 2007.

44 Van Hunnik E, Pots BFM, Hendriksen ELJA. The formation of protective FeCO3 corrosion product layers in CO2 corrosion. Corrosion. 1996

45 Al-Hassan S, Mishra B, Olson DL, Salama MM. Effect of microstructure on corrosion of steels in aqueous solutions containing carbon dioxide. Corrosion. 1998;54(6):480-491. http://dx.doi.org/10.5006/1.3284876.

46 Lopez DA, Schreiner WH, de Sánchez SR, Simison SN. The influence of carbon steel microstructure on corrosion layers: an XPS and SEM characterization. Applied Surface Science. 2003;207(1-4):69-85. http://dx.doi.org/10.1016/S0169-4332(02)01218-7.

47 Báez V, Vera J. Electrochemical noise for evaluating pitting resistance of cra materials under simulated well conditions. Corrosion. 2001

48 Kowaka M, Nagata S. Stress corrosion cracking of mild and low alloy steels in CO-CO2-H2O environments. Corrosion. 1976;32(10):395-401. http://dx.doi.org/10.5006/0010-9312-32.10.395.

49 Boven G, Chen W, Rogge R. The role of residual stress in neutral pH stress corrosion cracking of pipeline steels. Part I: PItting and cracking occurrence. Acta Materialia. 2007;55(1):29-42.

50 Raja VS. Stress corrosion cracking: theory and practice. Sawston, Cambridge: Woodhead Publishing; 2011.

51 Beavers JA, Johnson JT, Sutherby RL. Materials factors influencing the initiation of near-neutral pH soil environments. In: Proceedings of the 3rd International Pipeline Conference Calgary; 2000; Alberta, Canada. USA: ASME; 2000.

52 Wu S, Chen H, Ramandi H, Hagan PC, Crosky A, Saydam S. Effects of environmental factors on stress corrosion cracking of cold-drawn high-carbon steel wires. Corrosion Science. 2018;132:234-243. http://dx.doi.org/10.1016/j.corsci.2017.12.014.

53 Chen W, Vanboven G, Rogge R. The role of residual stress in neutral pH stress corrosion cracking of pipeline steels – Part II: crack dormancy. Acta Materialia. 2007;55(1):43-53. http://dx.doi.org/10.1016/j.actamat.2006.07.021.

54 Beavers JA, Johnson JT, Sutherby RL. Materials factors influencing the initiation of near-neutral pH SCC on underground pipelines. In: Proceedings of 3rd International Pipeline Conference; 2000 Oct 1-5; Calgary, Canada. Calgary, Canada: International Petroleum Technology Institute; 2000. p. 979.

55 Liu R, Cui L, Liu L, Zhang B, Wang F. A primary study of the effect of hydrostatic pressure on stress corrosion cracking of Ti-6Al-4V alloy in 3.5% NaCl solution. Corrosion Science. 2020;165:108402.

56 Yang ZX, Kan B, Li JX, Su YJ, Qiao LJ. Hydrostatic pressure effects on stress corrosion cracking of X70 pipeline steel in a simulated deep-sea environment. International Journal of Hydrogen Energy. 2017;42(44):27446-27457. http://dx.doi.org/10.1016/j.ijhydene.2017.09.061.

57 Schmitt G. Fundamental aspects of CO2 corrosion. Advances in CO2 corrosion. San Diego: NACE International; 1984.

58 Nguyen T, Bolivar J, Shi Y, Réthoré J, King A, Fregonese M, et al. A phase field method for modeling anodic dissolution induced stress corrosion crack propagation. Corrosion Science. 2018;132:146-160. http://dx.doi.org/10.1016/j.corsci.2017.12.027.

59 Burleigh T. The postulated mechanisms for stress corrosion cracking of aluminum alloys: a review of the literature 1980–1989. Corrosion. 1991;47(2):89-98. http://dx.doi.org/10.5006/1.3585235.

60 Lynch SP. Mechanistic and fractographic aspects of stress-corrosion cracking (SCC). In: Raja VS, Shoji T, editors. Stress corrosion cracking: theory and practice. Sawston, Cambridge: Woodhead Publishing; 2011.

61 Lynch SP. Hydrogen embrittlement (HE) phenomena and mechanisms. In: Raja VS, Shoji T, editors. Stress corrosion cracking: theory and practice. Sawston, Cambridge: Woodhead Publishing; 2011. http://dx.doi.org/10.1533/9780857093769.1.90.

62 Robertson IM, Sofronis P, Nagao A, Martin ML, Wang S, Gross DW, et al. Hydrogen embrittlement understood. Metallurgical and Materials Transactions. A, Physical Metallurgy and Materials Science. 2015;46(6):2323-2341. http://dx.doi.org/10.1007/s11661-015-2836-1.

63 Kamoutsi H, Haidemenopoulos GN, Bontozoglou V, Pantelakis S. Corrosion-induced hydrogen embrittlement in aluminum alloy 2024. Corrosion Science. 2006;48(5):1209-1224. http://dx.doi.org/10.1016/j.corsci.2005.05.015.

64 Parkins RN. Environmentally assisted cracking test methods. In: Cottis B, Graham M, Lindsay R, Lyon S, Richardson T, Scantlebury D, Stott H. Shreir's corrosion. USA: Elsevier; 2010. http://dx.doi.org/10.1016/B978-044452787-5.00181-5.

65 Dietzel W, Bala Srinivasan P, Atrens A. Testing and evaluation methods for stress corrosion cracking (SCC) in metals. In Raja VS, Shoji. T. Stress corrosion cracking: theory and practice. Sawston, Cambridge: Woodhead Publishing. Woodhead Publishing Series in Metals and Surface Engineering.

66 ASTM International. ASTM-G49. Standard Practice for Preparation and Use of Direct Tension Stress-Corrosion Test Specimens. West Conshohocken, PA: ASTM International; 2019.

67 ASTM International. ASTM-G39. Standard Practice for Preparation and Use of Bent-Beam Stress-Corrosion Test Specimens. West Conshohocken, PA: ASTM International; 2016.

68 American National Standards Institute. NACE-TM-0177. Laboratory Testing of Metals for Resistance to Sulfide Stress Cracking and Stress Corrosion Cracking in H2S Environments. Washington: ANSI; 2016.

69 International Organization for Standardization. ISO-7539-2. Corrosion of metals and alloys — Stress corrosion testing — Part 2: Preparation and use of bent-beam specimens. Genebra: ISO; 1989.

70 Scully JR, Moran P. Influence of strain on hydrogen assisted cracking of cathodically polarized high-strength steel. In Lisagor W, Crooker T, Leis B. Environmentally assisted cracking: science and engineering - ASTM STP 1049. West Conshohocken, PA: ASTM International; 1990. http://dx.doi.org/10.1520/STP24058S.

71 ASTM International. ASTM-G129. Standard Practice for Slow Strain Rate Testing to Evaluate the Susceptibility of Metallic Materials to Environmentally Assisted Cracking. West Conshohocken, PA: ASTM International; 2013.

72 ASTM International. ASTM-F1624. Standard Test Method For Measurement Of Hydrogen Embrittlement Threshold In Steel By The Incremental Step Loading Technique. West Conshohocken, PA: ASTM International; 2018.

73 Dietzel W, Turnbull A. Stress corrosion cracking. In: Milne I, Ritchie RO, Karihaloo B, editors. Comprehensive structural integrity. USA: Elsevier; 2007.

74 Hudgins C, McGlasson R, Mehdizadeh P, Rosborough W. Hydrogen sulfide cracking of carbon and alloy steels. 1966;22(8):231-251.